

Lumbar Spine Degenerative Classification

Hammad Aamer (4732728, Masters in Data and Computer Science) June 1, 2025

Abstract

This project focuses on developing a deep learning model capable of accurately identifying and localizing key anatomical features in spinal MRI images, using a dataset enriched with Object-Centered Pose-Centric (OCPC) heatmaps. Our primary objective was to detect spinal abnormalities, such as degenerative conditions, and pinpoint key spinal landmarks in the images. The model input consists of preprocessed DICOM images, accompanied by heatmaps and offset vectors to aid in accurate localization.

The model employs a convolutional neural network (CNN) as the primary feature extractor, followed by specialized layers for heatmap generation and offset prediction. It outputs probability heatmaps highlighting the likelihood of specific spinal abnormalities at different points in the image, along with spatial offsets for refined localization. By combining classification and spatial offset prediction, our approach offers a robust, accurate means for analyzing spinal images, which could support automated medical diagnosis and aid radiologists in assessing spinal conditions with improved precision.

1. Introduction

Classifying diseases based on imaging data, such as MRI scans, is a critical task in medical diagnostics. With the advancement of machine learning algorithms, computers are increasingly handling this role with promising accuracy. Automated spinal analysis can benefit healthcare significantly, aiding early detection and personalized treatment plans while reducing radiologists' workload.

In this project, we aim to classify lumbar spine degenerative conditions by replicating the methodology from the paper [1]. We utilize a DeepLabv3+ architecture with a ResNet backbone to generate pixel-wise segmentation and classification maps. Before detailing the technical implementation, we provide foundational insights into the types of spinal degeneration and relevant anatomical terminology. Understanding these conditions and anatomical structures is essential for the effective interpretation of MRI scans.

Imaging Overview

MRI imaging of the spine captures views in three planes: axial, sagittal, and coronal. Each plane offers unique in-

sights:

- The **Axial** plane provides cross-sections of the spine from top to bottom, perpendicular to the spine's length. This view is essential for assessing conditions like canal stenosis and foraminal narrowing.
- The **Sagittal** plane offers side-to-side slices, allowing visualization along the spine's length, crucial for observing overall spine alignment and intervertebral disc spaces.
- The **Coronal** plane offers a front-to-back view, though less commonly used for lumbar degeneration analysis.

MRI images are further classified as T1 or T2 weighted. T1 images highlight fat (making the inner part of bones appear bright), providing detailed anatomical structures, while T2 images make water appear bright, enhancing visibility of the spinal canal and intervertebral discs. Unlike CT scans, MRI images lack standardized pixel intensities, which can introduce challenges in model generalization.

Anatomical Overview

The spine is a complex structure divided into four main regions: the cervical (7 vertebrae), thoracic (12 vertebrae), lumbar (5 vertebrae), and sacral (3-5 fused vertebrae). Each region has unique characteristics and functions:

- The **Cervical** spine supports the head and allows for a range of motion.
- The **Thoracic** spine provides stability and attaches to the ribcage.
- The **Lumbar** spine bears the weight of the upper body and is most susceptible to degeneration due to high loads.
- The **Sacral** spine connects to the pelvis, providing structural support.

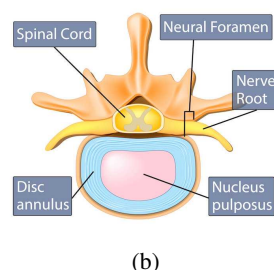
Intervertebral discs act as shock absorbers between each vertebral body (except in the sacral region). The spinal cord runs along the posterior of each vertebra, with spinal nerves exiting through foramina. An anatomical overview of the spine is shown in Figure 1.

Overview of Degenerative Conditions

Compression of the spinal cord or surrounding nerves can cause pain and discomfort. This compression may result from factors such as bulging intervertebral discs, bone degeneration, trauma, or thickened ligaments. Below, we introduce key degenerative conditions affecting the spine, each with distinct anatomical implications.

108
109
110
111
112
113
114
115
116
117
118

(a)



(b)

Figure 1: Anatomical overview of a) spine and b) vertebral disc

Foraminal Narrowing

Foramina are the openings through which spinal nerves exit the spinal canal. Compression of these openings, known as foraminal narrowing, can lead to pain along the affected nerve path and potential motor or sensory deficits. This condition is often associated with age-related disc degeneration or bony outgrowths (osteophytes). The sagittal plane is particularly useful for detecting foraminal narrowing, as illustrated in Figure 2.

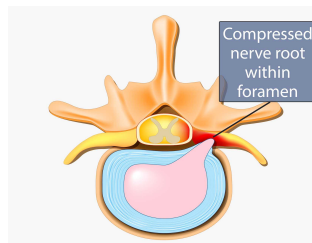


Figure 2: Illustration of foraminal narrowing

Subarticular Stenosis

Subarticular stenosis is similar to foraminal narrowing but affects the lateral recess area, located between the spinal canal and nerve root pathway. This narrowing can compress the spinal cord or nerve roots, leading to neurological symptoms. Subarticular stenosis can be challenging to diagnose due to the small spaces involved and the lack of standardized diagnostic criteria.

Canal Stenosis

Canal stenosis refers to the narrowing of the spinal canal, which can compress the spinal cord and cause significant symptoms, including back pain, tingling, and muscle weakness. This condition is commonly visualized in the axial plane and is often associated with degenerative changes like

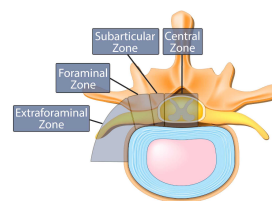
162
163
164
165
166
167
168
169
170
171

Figure 3: Illustration of herniation zones

172
173
174
175
176
177
178
179
180
181
182
183
184
185
186
187
188
189
190

ligament thickening, disc herniation, or osteophyte formation.



Figure 4: Example of canal stenosis

2. Dataset

The dataset, obtained from the RSNA 2024 Lumbar Spine Degenerative Classification competition on Kaggle, is curated specifically for analyzing degenerative lumbar spine conditions via MRI imaging. It consists of multiple structured files that provide a wealth of clinical information for model training and testing.

The main dataset file, **train.csv**, contains severity labels for various spinal conditions at different vertebral levels, including conditions like

spinal_canal_stenosis_11_12. Each condition is categorized into three levels of severity: Normal/Mild, Moderate, and Severe. The **train.csv** file ties each condition to a unique identifier, the **study_id**, allowing multiple image series (MRI sequences) to be grouped under the same clinical study. This structure simulates real-world clinical scenarios where a patient undergoes multiple imaging sequences.

A crucial component for spatial analysis is the **train_label_coordinates.csv** file, which provides (x, y) coordinate labels pinpointing specific conditions within each MRI study. This file also contains identifiers for **series_id** and **instance_number**, which enable the precise location of individual images in the MRI scan stack. Conditions

such as spinal canal stenosis, neural foraminal narrowing, and subarticular stenosis are evaluated bilaterally across vertebral levels, including I3.I4, with x, y coordinates for targeted localization.

Further metadata is contained in the `train_series.descriptions.csv` file, which specifies the MRI sequence type for each image series within a study. MRI sequences include **Sagittal T2/STIR**, **Sagittal T1**, and **Axial T2**. This metadata assists in understanding the imaging modality, enabling models to leverage modality-specific features in analysis.

The dataset's image files are organized into a directory structure defined by `study_id/instance_id/img_id` and stored in DICOM (.dcm) format, preserving both spatial details and metadata for each scan. In this work, we focus on the **Sagittal T2/STIR** subset due to its high relevance for lumbar spine diagnostics, reducing data processing complexity while ensuring quality training data. This subset comprises 1,974 studies in total, offering a robust sample for training and evaluation. Together, these structured files provide a richly detailed dataset that combines clinical labels, precise spatial coordinates, and imaging metadata, supporting accurate localization and diagnosis of various spinal conditions.

3. Approach

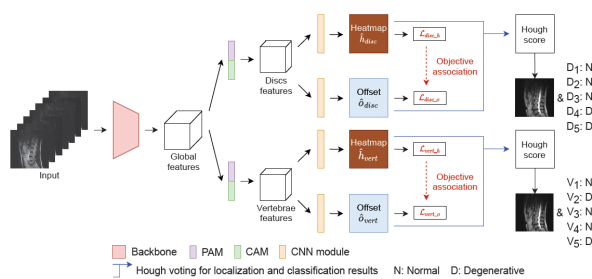


Figure 5: Sketch of our network architecture adapted from [1].

Our methodology closely follows the SpineOne approach, an efficient one-stage framework for automatically localizing and classifying degenerative discs and vertebrae in lumbar spine MRI scans. This framework addresses three primary challenges in spinal degeneration classification: (1) the simultaneous localization of multiple centroids alongside classification of degenerative conditions, (2) consistent classification across both discs and vertebrae despite structural similarities, and (3) the need for efficient multitasking between localization and classification objec-

tives.

SpineOne leverages convolutional neural networks (CNNs) to predict the spatial locations of disc and vertebral centroids (keypoints) while classifying their degeneration levels. This approach minimizes the annotation requirements typically needed for segmentation-based methods, thereby easing the workload for clinical annotators and enabling broader applicability.

To address the main challenges, three innovations are incorporated:

- One-Channel-Per-Class (OCPC) Keypoint Heatmap:** This method enables simultaneous localization and classification by encoding both spatial and classification information into a single heatmap, which simplifies the network architecture while maintaining classification accuracy.
- Dual Self-Attention Modules:** The model incorporates Position Attention Module (PAM) and Channel Attention Module (CAM) mechanisms to enhance feature integration across both positional and channel dimensions. These attention modules are inspired by the way radiologists interpret MRI slices, synthesizing both localized and broader features.
- Gradient-Guided Objective Association (OA):** This mechanism is a critical component of the SpineOne framework, facilitating the concurrent learning of localization and classification tasks. For both discs and vertebrae, the model generates keypoint heatmaps to identify key locations and offsets to refine these locations. By guiding the offset learning process with gradients from the heatmap loss, the OA mechanism enhances model performance, especially in later training stages, by reinforcing the correlation between heatmap accuracy and offset values. This complementary interaction between heatmaps and offsets boosts the model's effectiveness in both localization and classification tasks.

Our approach differs from the original SpineOne model in several key aspects. Unlike the original model, which includes both spine and vertebrae keypoints, our dataset only includes vertebrae keypoints. Additionally, our severity levels expand upon the original binary classification (Normal vs. Degenerative) by incorporating a third class, resulting in three severity levels (Normal/Mild, Moderate, Severe). This necessitates adjustments to our output channels: instead of two output channels for the two original heatmap heads, our model uses three channels for the single heatmap head to accommodate the additional severity class. Furthermore, we reduced the offset head

324 configuration to just one head producing three coordinates,
 325 totaling six channels (one coordinate for each severity)
 326 instead of two heads as in SpineOne.
 327

328 By adopting a single-stage design, our framework
 329 efficiently produces both localization and classification
 330 results, making it suitable for clinical use. The model out-
 331 puts centroids, offset values, and pixel-wise degeneration
 332 probabilities for each disc and vertebra, reducing manual
 333 effort and potentially improving diagnostic accuracy by
 334 highlighting key areas for attention in spinal MRI scans.
 335

337 4. Data Preprocessing

338 Data preprocessing is crucial to ensure that the model
 339 ingests well-structured inputs. Here, we prepared both
 340 annotation and image data by generating heatmaps and
 341 offset maps to facilitate the model’s learning of key points
 342 of interest in spinal images. Initially, the dataset included
 343 multiple annotation files, detailing severity levels, image
 344 coordinates, and MRI series descriptions. These files were
 345 merged based on common `study_id` fields, creating a
 346 unified dataset for training. Each annotation was mapped
 347 to its corresponding heatmap and offset, precomputed for
 348 efficiency during model training.
 349

350 Since the dataset’s images varied in dimensions, all
 351 images were resized to a fixed 512x512 resolution to
 352 maintain uniformity during training. Keypoint coordinates
 353 were proportionally adjusted to match the resized images,
 354 ensuring accurate representation within the One-Channel-
 355 Per-Class (OCPC) heatmaps.
 356

357 Heatmaps were generated by assigning pixel values of
 358 1 around each keypoint within a specified radius (set at
 359 6 pixels following the SpineOne paper’s methodology).
 360 However, it is to be noted that 6 pixels may cover a larger
 361 or smaller body area based on the resolution of the image.
 362 As such, since we had to work with limited processing
 363 capabilities our smaller image resolution means a 6 pixel
 364 radius is a significantly larger area of the body for our
 365 project, and as such a greater emphasis is on the accuracy
 366 of our offset for accurate localization of disformity. Offset
 367 maps were created to represent each pixel radius’s relative
 368 position to its nearest keypoint, resized for consistency
 369 across the dataset. This preprocessing helped the model
 370 learn spatial locations and keypoint classifications in
 371 tandem.
 372

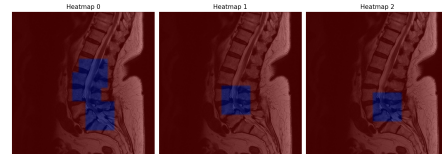
373 The target heatmaps and offsets were constructed with
 374 the following dimensions:
 375

- 376 • **Heatmap:** 3 channels (one per severity level).

- 377 • **Offsets:** 6 channels (2 for each severity level, covering
 378 x and y dimensions).



379 Figure 6: Spine deformity of different severities overlaid
 380 on an image



381 Figure 7: Heatmap targets with a 6 pixel radius window

388 5. Model Pipeline

389 The model pipeline integrates several components de-
 390 signed to localize and classify degenerative conditions in
 391 lumbar spine MRI images effectively.
 392

393 5.1. Backbone: Feature Extraction

394 Our model’s backbone leverages the DeepLabV3 archi-
 395 tecture, which uses a ResNet-50 base optimized for image
 396 segmentation. To accommodate single-channel grayscale
 397 MRI images, we modified ResNet-50’s initial convolutional
 398 layer, adapting the model to this specific input while retain-
 399 ing the feature richness learned from pretraining. The back-
 400 bone captures essential low-level details (e.g., edges and
 401 textures), enabling accurate keypoint localization within
 402 MRI scans.
 403

404 5.1.1 Position Attention Module (PAM)

405 The Position Attention Module (PAM) plays a key role by
 406 capturing long-range spatial dependencies in the MRI im-
 407 ages. PAM computes weighted sums of features across all
 408 image positions, focusing the model’s attention on spatially
 409 relevant structures such as discs and vertebrae. While PAM
 410 can be computationally demanding for high-resolution im-
 411 ages, its capacity for spatial focus enhances model per-
 412 formance in localizing critical structures. Figure 8 illus-
 413 trates the PAM’s configuration as outlined in the SpineOne
 414 paper.
 415

416 5.1.2 Channel Attention Module (CAM)

417 Complementing PAM, the Channel Attention Module
 418 (CAM) emphasizes interdependencies among different
 419

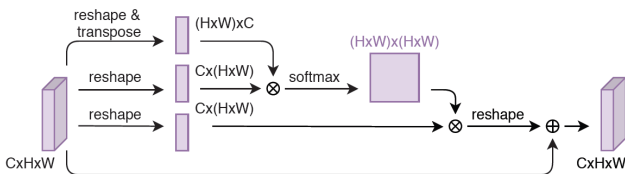


Figure 8: Structure of the Position Attention Module

feature channels. CAM highlights features essential for identifying disc and vertebra abnormalities by integrating across channels, improving efficiency compared to PAM in memory usage. The combined strengths of PAM and CAM enable a balanced capture of spatial and feature-level patterns, which enriches the model's representation of lumbar degenerative conditions. Figure 9 shows the CAM's structure.

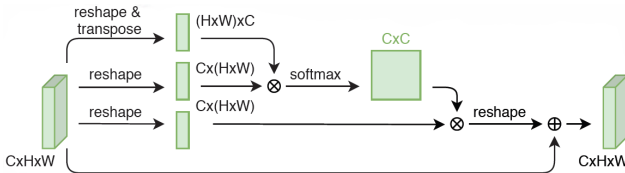


Figure 9: Structure of the Channel Attention Module

5.2. Heatmap Head

The heatmap head outputs a spatial probability map for each class (Normal/Mild, Moderate, Severe), indicating the probability that each pixel represents a specific class. This helps in pinpointing the locations of vertebrae and discs by assigning probabilities to regions of interest.

5.3. Offset Head

The offset head calculates 2D displacement vectors relative to each keypoint, outputting a vector field in both x and y directions. This assists the model in refining keypoint locations by predicting how far each pixel lies from its closest keypoint.

5.4. Heatmap-Offset Fusion

The heatmap and offset outputs are fused to finalize keypoint locations and their associated classes. This integration optimizes both spatial predictions and class identification, supporting the model's ability to deliver a well-rounded anatomical representation in MRI images.

5.5. Objective Association

The OA mechanism refines the offset loss by incorporating gradient information from the heatmap loss. Taking the

disc structure as an example, the OA mechanism redefines its loss as:

$$L_{\text{disc}} = L_{\text{disc}}^h + L_{\text{disc}}^o \left(R \left(1 \oplus \frac{\partial L_{\text{disc}}^h}{\partial \hat{h}_{\text{disc}}} \right) \odot \hat{o}_{\text{disc}}, o_{\text{disc}} \right)$$

where:

- $\frac{\partial L_{\text{disc}}^h}{\partial \hat{h}_{\text{disc}}}$ is the gradient of the heatmap loss with respect to the predicted heatmap, highlighting regions that are crucial for both localization and classification.
- $R(\cdot)$ adjusts the tensor dimensions for compatibility in element-wise operations.
- $1 \oplus \frac{\partial L_{\text{disc}}^h}{\partial \hat{h}_{\text{disc}}}$: This element-wise addition combines a constant tensor with the gradient, ensuring contributions from all regions while emphasizing high-importance areas.
- The element-wise product (\odot) focuses offset learning on pixels that the heatmap deems most significant for localization.

5.5.1 Gradient Clipping and Practical Application

To maintain stable learning, the gradient values are clipped between $[-100, 100]$ and normalized to a range of $[0, 1]$. Applying the OA mechanism in later training stages, once the model's structure has stabilized, helps to fine-tune performance using this scaled information.

6. Loss Function

6.1. Heatmap Loss

Binary Cross-Entropy (BCE) loss measures accuracy in heatmap predictions, comparing the model's output with the ground truth to improve spatial probability mapping. Focal Loss is based on BCE but designed to give more weight to hard-to-classify examples since most of our dataset consists of mild cases. It is calculated using:

$$\text{FL}(\hat{p}) = -(1 - \hat{p})^\gamma \log(\hat{p})$$

6.2. Offset Loss

The Mean Absolute Error (MAE) loss, also known as L1 loss evaluates the discrepancy between predicted and true offsets, guiding the model toward accurate keypoint predictions.

6.3. Total Loss

Total loss combines BCE and MSE in a weighted fashion, balancing localization and classification objectives to enhance model performance for identifying degenerative

540 spinal conditions. It is constructed from four main loss
541 terms, divided between discs and vertebrae:
542

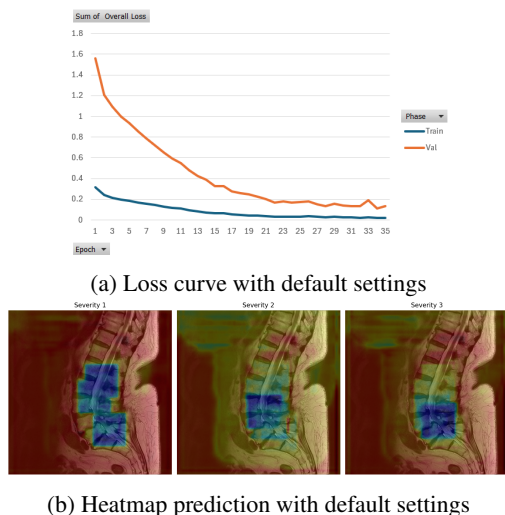
$$543 L = L_{\text{disc}}^h + L_{\text{disc}}^o + L_{\text{vert}}^h + L_{\text{vert}}^o$$

545 where L_{disc}^h and L_{vert}^h represent the heatmap losses for discs
546 and vertebrae, while L_{disc}^o and L_{vert}^o correspond to the offset
547 losses.

548 7. Experiments

549 7.1. Default Settings

550 Our experiments began with training the model under
551 conditions closely resembling those specified in the SpineOne
552 paper. This setup included simultaneous training
553 on both the heatmap and offset predictions, along with the
554 use of both Position Attention Module (PAM) and Channel
555 Attention Module (CAM) throughout training. However,
556 due to hardware limitations, we had to make certain
557 modifications to the original setup. Notably, we excluded
558 Objective Association (OA) between the loss functions,
559 which the paper suggests adding only after about 80% of
560 training epochs. Despite this deviation, the model achieved
561 favorable results, likely due to the limited influence OA
562 was expected to exert in early epochs.
563



582 Figure 10: Comparison of Loss Curve and Heatmap Prediction
583 with Default Settings

584 We also resized input images to 512x512 pixels to
585 ensure efficient training on available hardware. This
586 resizing proved beneficial for resource management while
587 maintaining satisfactory model performance. Loss curves
588 and prediction results are provided below to illustrate
589 the model’s learning trajectory. For all experiments, we
590 used a confusion matrix to assess model performance.
591

592 Due to three severity classes in the dataset, we grouped
593 the Moderate and Severe classes into a single "Positive"
594 category, while classifying the Normal class as "Negative."
595

596 The confusion matrix and key metrics (accuracy and F1
597 score) for this experiment are presented in Table 1. Results
598 indicate that the model successfully learned to differentiate
599 classes with a moderate level of accuracy, although there
600 were relatively high false positives and false negatives.
601

602 Table 1: Confusion Matrix with Accuracy Metrics

	Actual Positive	Actual Negative
Predicted Positive	7 (TP)	17 (FP)
Predicted Negative	11 (FN)	65 (TN)
<hr/>		
Metric	Value	
Accuracy		611
F1 Score		612

613 The results from the default settings show moderate
614 success in differentiating between severity classes. The
615 model’s accuracy of 72% indicates good overall perfor-
616 mance, though the F1 score of 0.33 reflects a need for bet-
617 ter handling of class imbalances, particularly in identifying
618 Positive cases.
619

620 7.2. Ablation Studies

621 To better understand the contributions of each compo-
622 nent in the model, we performed ablation studies by selec-
623 tively omitting different elements during training.
624

625 7.2.1 Exclusion of Offset Loss

626 Our first ablation experiment removed the offset loss from
627 training. The goal was to test if the model could main-
628 tain robust performance by focusing solely on heatmap
629 predictions. This setup was hypothesized to retain the
630 severity classification accuracy, as practitioners could still
631 benefit from precise heatmap localization, even without
632 offset-based adjustments. Loss curves and prediction
633 visualizations are shown in Figure 11.
634

635 The confusion matrix and metrics for this experiment
636 are shown in Table 2. With offset loss excluded, the
637 model achieved a higher accuracy of 77% and an improved
638 F1 score of 0.43, suggesting that concentrating solely
639 on heatmap predictions may lead to stronger severity
640 classification results under certain conditions.
641

642 These results suggest that, by eliminating offset loss, the
643 model managed to achieve better balance between precision
644 and recall.
645

648
649
650
651
652
653
654
655
656
657
658
659
660
661
662
663
664
665
666
667
668
669
670
671
672
673
674
675
676
677
678
679
680
681
682
683
684
685
686
687
688
689
690
691
692
693
694
695
696
697
698
699
700
701

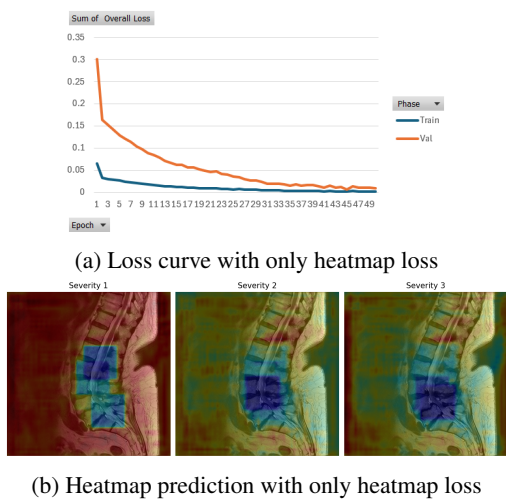


Figure 11: Comparison of Loss Curve and Heatmap Prediction with only heatmap loss

Table 2: Confusion Matrix and Accuracy Metrics (Offset Loss Excluded)

	Actual Positive	Actual Negative
Predicted Positive	9 (TP)	14 (FP)
Predicted Negative	9 (FN)	68 (TN)
	Metric	Value
Accuracy	0.77	
F1 Score	0.43	

and recall. This highlights the potential utility of heatmap-only predictions for clinical settings, where quick and accurate identification of degenerative severity levels could outweigh the benefits of fine-grained localization.

7.2.2 Exclusion of Attention Modules (PAM and CAM)

The next ablation focused on removing the PAM and CAM modules to assess the impact of attention mechanisms on model performance. Removing these modules resulted in a simpler architecture, which we hypothesized might impact both classification and localization accuracy due to the loss of spatial and feature-channel attention.

Table 3 presents the confusion matrix and metrics for this experiment. The accuracy dropped to 69%, and the F1 score was reduced to 0.28, indicating a decline in the model's ability to differentiate between severity classes without attention mechanisms.

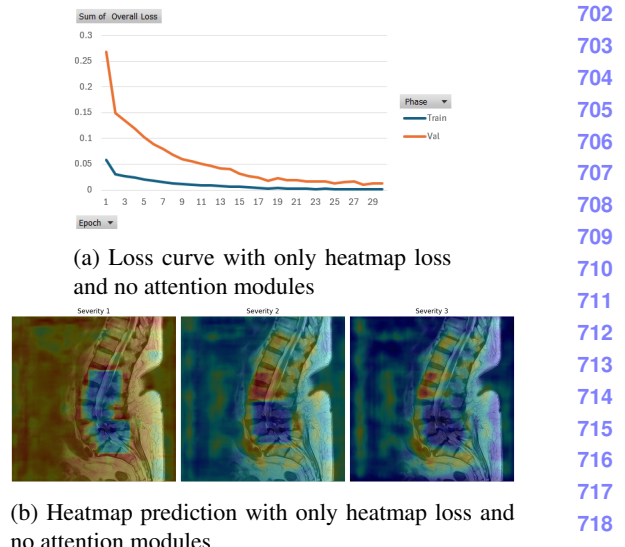


Figure 12: Comparison of Loss Curve and Heatmap Prediction with only heatmap loss and no attention modules

Table 3: Confusion Matrix and Accuracy Metrics (Attention Modules Excluded)

	Actual Positive	Actual Negative
Predicted Positive	6 (TP)	19 (FP)
Predicted Negative	12 (FN)	63 (TN)
	Metric	Value
Accuracy	0.69	
F1 Score	0.28	

The decrease in accuracy and F1 score underlines the importance of attention mechanisms, particularly in complex tasks like spine image classification. The absence of PAM and CAM significantly impacted the model's precision and recall, demonstrating that attention modules are essential for capturing the spatial and channel-based dependencies that contribute to accurate localization and classification.

7.3. Summary of Results

The ablation studies reveal the following insights:

- Offset Loss Impact:** Excluding the offset loss improved the model's classification metrics, suggesting that focusing on heatmap accuracy alone may yield substantial benefits for classification tasks, particularly in settings prioritizing severity prediction over precise localization.
- Attention Modules Impact:** Removing PAM and CAM led to a notable decline in accuracy and F1 score.

756	underscoring their value in capturing complex spatial	810
757	and feature-level relationships that are crucial for dis-	811
758	tinguishing spinal degenerative conditions.	812
759		813
760	In summary, the default model settings provided bal-	814
761	anced performance across both localization and classifi-	815
762	cation tasks. However, alternative configurations such as	816
763	heatmap-only training and the inclusion of attention mod-	817
764	ules can further optimize the model based on specific appli-	818
765	cation needs.	819
766		820
767	8. Conclusion	821
768		822
769	In this report, we explored the effectiveness of our	823
770	model in predicting spinal deformities by replicating the	824
771	work presented in the SpineOne paper. Through a series	825
772	of experiments and ablation studies, we demonstrated that	826
773	our model can accurately classify severity levels of spinal	827
774	conditions using heatmap and offset predictions.	828
775		829
776	Our results indicate that, even without certain elements	830
777	such as the Objective Association (OA) and attention	831
778	mechanisms, the model performed reasonably well. The	832
779	omission of OA and a focus on heatmap accuracy led to	833
780	an improved classification accuracy of 77% when offset	834
781	loss was excluded. This suggests that the model can still	835
782	provide valuable insights for practitioners, even when	836
783	certain components are not fully utilized.	837
784		838
785	Moreover, the significant drop in performance when	839
786	excluding the Position Attention Module (PAM) and Chan-	840
787	nel Attention Module (CAM) highlighted the importance	841
788	of these mechanisms in enhancing the model's ability to	842
789	capture critical spatial and feature dependencies within	843
790	the data. Their contribution was crucial for maintaining a	844
791	balanced performance across precision and recall metrics,	845
792	which are essential in clinical applications.	846
793		847
794	Overall, our findings affirm the potential of the proposed	848
795	model for clinical utility in diagnosing and assessing spinal	849
796	deformities. Future work could further optimize the archi-	850
797	ecture and explore the integration of additional data modal-	851
798	ties to improve predictive accuracy and robustness. The	852
799	insights gleaned from this study pave the way for enhanced	853
800	diagnostic tools in the field of spinal health, emphasizing	854
801	the necessity for continued research and development in this	855
802	area.	856
803		857
804	References	858
805	[1] Jiabo He, Wei Liu, Yu Wang, Xingjun Ma, and Xian-Sheng	859
806	Hua. <i>SpineOne: A One-Stage Detection Framework for De-</i>	860
807	<i>generative Discs and Vertebrae</i> . 2021. 1, 3	861
808		862
809		863